Astron. Astrophys. 329, 399–408 (1998)

ASTRONOMY AND ASTROPHYSICS

Dust in high-z radio-loud AGN*

A. Cimatti[1], **W. Freudling**[2,3], **H.J.A. Röttgering**[4], **R.J. Ivison**[5], **and P. Mazzei**[6]

[1] Osservatorio Astrofisico di Arcetri, Largo E. Fermi 5, I-50125 Firenze, Italy
[2] European Southern Observatory, Karl-Schwarzschild-Str. 2, D-85748 Garching, Germany
[3] Space Telescope, European Coordinating Facility, Karl-Schwarzschild-Str. 2, D-85748 Garching, Germany
[4] Sterrewacht, Huygens Lab., P.O. Box 9513, 2300 RA Leiden, The Netherlands
[5] Institute for Astronomy, University of Edinburgh, Royal Observatory, Blackford Hill, Edinburgh EH9 3HJ, UK
[6] Osservatorio Astronomico, Vicolo dell'Osservatorio 5, I-35122 Padova, Italy

Received 20 May 1997 / Accepted 7 August 1997

Abstract. We present continuum observations of a small sample of high-redshift, radio-loud AGN (radio galaxies and quasars) aimed at the detection of thermal emission from dust. Seven AGN were observed with IRAM and SEST at 1.25 mm; two of them, the radio galaxies 1243+036 ($z \sim 3.6$) and MG 1019+0535 ($z \sim 2.8$) were also observed at 0.8 mm with the JCMT submillimetre telescope. Additional VLA observations were obtained in order to derive the spectral shape of the synchrotron radiation of MG 1019+0535 at high radio frequencies. MG 1019+0535 and TX 0211−122 were expected to contain a large amount of dust based on their depleted Lyα emission. The observations suggest a clear 1.25-mm flux density excess over the synchrotron radiation spectrum of MG 1019+0535, suggesting the presence of thermal emission from dust in this radio galaxy, whereas the observations of TX 0211−122 were not sensitive enough to meaningfully constrain its dust content. On the other hand, our observations of 1243+036 provide a stringent upper limit on the total dust mass of $< 10^8\,M_\odot$. Finally, we find that the spectra of the radio-loud quasars in our sample ($2 < z < 4.5$) steepen between rest-frame radio and the far-infrared. We discuss the main implications of our results, concentrating on the dusty radio galaxy, MG 1019+0535.

Key words: galaxies: active – galaxies: ISM – radio continuum: galaxies – quasars: general – galaxies: G 1243+036; MG 1019+0535

1. Introduction

In recent years several attempts have been made to study the interstellar medium in high-redshift galaxies. Promising results have been obtained by millimetre and submillimetre observations, which sample the rest-frame far-IR emission of galaxies at $z > 2$ (Andreani et al. 1993). The study of dust in distant galaxies is very important because it provides information on the physical state of the ISM, and its relation to other properties of the galaxies, such as activity and evolution. For example, if it is correct to assume that the rest-frame far-IR luminosity $L_{\rm FIR}$ is a measure of the star-formation rate, then this could provide a way to estimate the evolutionary state of high-z galaxies. Establishing whether dusty galaxies are common at high redshifts is also important in order to evaluate the effects of dust obscuration on surveys of quasars and protogalaxies carried out in optical bands (Smail, Ivison & Blain 1997).

Several active galaxies with $z > 2$ have been detected in submillimetre/millimetre bands, suggesting the presence of large amounts of dust in their host galaxies ($M_{\rm d} \sim 10^{8-9}\,M_\odot$; see Hughes, Dunlop & Rawlings 1997 for a recent review; Omont et al. 1996b; Ivison et al. 1998). At high redshift, dust is also thought to be present in damped Lyα absorption systems (Pettini et al. 1994; Pei, Fall & Bechtold 1991), in very red galaxies (Hu & Ridgway 1994), and in high-z radio galaxies (Cimatti 1996 and references therein). A substantial amount of dust is also expected in theoretical models of the evolution of galaxies at high-z (Mazzei & De Zotti 1996 and references therein). Finally, it is important to recall that molecular gas has been observed in a few distant active galaxies, allowing a direct estimate of the dust-to-gas mass ratio at large cosmological distances for the first time (see Omont et al. 1996a; Ohta et al. 1996).

We recall that particular caution is needed in the interpretation of the submillimetre/millimetre data of radio-loud objects. The existence of a thermal dust emission excess should be confirmed by checking whether the submillimetre/millimetre flux densities represent a real excess over the synchrotron spectrum. The radio galaxy B2 0902+343 ($z \sim 3.4$) is an example of the problem, where the observed 1.3-mm flux density is not due to thermal emission from dust, but to the tail of the radio synchrotron spectrum (Downes et al. 1996 and references therein).

Send offprint requests to: A. Cimatti

* Partially based on observations obtained at the European Southern Observatory, La Silla, Chile

Therefore, high-frequency ($\sim 8 - 43$ GHz) radio observations are extremely important to derive the shape of the synchrotron spectrum and to estimate its contribution to the millimetre region.

In the present paper we present the results of millimetric observations of a small sample of radio galaxies and radio-loud quasars with $z > 2$, and additional high-frequency VLA observations of MG 1019+0535, a radio galaxy at $z \sim 2.8$. Throughout this paper we assume $H_0 = 50\,\mathrm{km\,s^{-1}\,Mpc^{-1}}$, $q_0 = 0.5$ and define $h_{50} = H_0/50$.

2. Observations and data reduction

We have observed seven objects with $2 < z < 4.5$; four radio galaxies and three radio-loud quasars. Table 1 shows the target details. The radio galaxies TX 0211−122 and MG 1019+0535 were observed because their UV spectra are suggestive of extinction by dust (van Ojik et al. 1994; Dey et al. 1995), MRC 0943−242 because of the the presence of a large amount of neutral hydrogen surrounding the host galaxy (Röttgering et al. 1995) and 1243+036 because of its very high redshift (van Ojik et al. 1996). Among the quasars, we recall that PKS 1251−407 is, to date, the most distant known radio-loud quasar (Shaver, Wall & Kellermann 1996). MRC 1043−291 (Kapahi et al. 1997) and PKS 1354−107 (Shaver et al. 1997, in preparation), were selected because of their convenient observability during the observing run.

2.1. SEST observations

The observations with the 15-m SEST (Swedish-ESO Submillimetre Telescope) were made at La Silla, Chile, during 1995 July and 1996 May. The telescope was equipped with a ^{3}He-cooled 1.3-mm bolometer, with a central frequency of 250 GHz and a bandwidth of around 50 GHz. The beamsize is about 24″ (FWHM) and the typical sensitivity is $200\,\mathrm{mJy\,s^{-1/2}}$. The observations were carried out during nights with rather low opacities. The opacity was checked by several skydips taken during the nights (i.e. the telescope was moved to six different elevations where the bolometer integrated for 10 s and a calculation of the zenith opacity was made). The pointing was checked using quasars as astrometric reference sources and the absolute flux calibration was achieved by observing the planet Uranus. We estimate that the flux calibration has a typical uncertainty of 20%. The observations were made in beam-switching mode with a beam throw of 70″, and the data were reduced according to method described by Andreani (1994) (see also Andreani et al. 1993). We have found a linear decrease of the standard deviation with $t^{-1/2}$, indicating that the observing conditions were stable and limited by the sky noise.

2.2. IRAM observations

Observations with the IRAM 30-m antenna were made in 1996 March with the MPIfR 1.3-mm 7-channel bolometer array. The bolometers are separated by 22″ in an hexagonal arrangement surrounding the central pixel. The individual beamsize is about 11″ (FWHM), and the typical sensitivity of $60\,\mathrm{mJy\,s^{-1/2}}$. The ON-OFF technique uses the wobbler with a beamthrow of 33″, integrating for 10 s per subscan. The opacity was monitored every 1-1.5 hr with a skydip procedure, and was around 0.4 during the first night and 0.2 during the second. In both cases, the atmosphere was quite stable. The flux calibration was achieved by observing Uranus, and the uncertainties are again of order 20%. The fluxes of the six outer channels were averaged and subtracted from the central channel.

2.3. JCMT observations

The radio galaxies 1243+036 and MG 1019+0535 were also observed at the JCMT (the 15-m James Clerk Maxwell Telescope, Mauna Kea, Hawaii) using the single-element ^{3}He-cooled UKT14 bolometer (Duncan et al. 1990), coupled with a broad-band filter (ν = 384 GHz; $\Delta\nu$ = 30 GHz FWHM). The observations were made using a 65-mm focal plane aperture, resulting in a FWHM beamwidth of 16.5″. Sky emission was subtracted by chopping the secondary mirror in azimuth, at a frequency of 7.8 Hz, with a throw of 60″.

The radio galaxy 1243+036 was observed on 1996 April 26 during excellent weather conditions. Calibration was taken from Mars (which set near the beginning of the shift) and the secondary calibrators NGC 2071IR, CRL 618, IRC +10216 (CW Leo) and 16293−2422. 3C 273 was used as a pointing source and bootstrap calibrator (observed eight times). The 384-GHz zenith optical depth was typically around 0.29, but it appeared to decrease towards the end of the shift (0.23). In total, 880 pairs of 16 s (i.e. 8 s in each beam) were obtained. The raw, uncalibrated dataset gave a S/N of 0.99. After despiking, calibration and statistical testing, the final result was 7.0 ± 3.1 mJy. The calibrated 800-μm flux of 3C 273 was 8.2 ± 0.1 Jy; IRC +10216 (which is variable) was 5.4 ± 0.1 Jy.

The radio galaxy MG 1019+0535 was observed over a period of 5.5 hr during 1996 April 24. A total of 3 hr was spent on-source, the remaining 2.5 hr being devoted to calibration. Flux calibration was provided by regular measurements of IRC +10216, as was a determination of the 375-GHz zenith opacity. Observations of local pointing sources kept rms pointing errors below 3″ and associated flux losses below 10%; the overall uncertainty in the flux measurement was therefore dominated by the poor S/N. After careful editing, the MG 1019+0535 measurements indicated a 375-GHz flux density of 14.7 ± 4.6 mJy – a marginal detection.

2.4. VLA observations

MG 1019+0535 was also observed at the Very Large Array (VLA), New Mexico. Radio continuum observations in the X (8.3 GHz), U (15.0 GHz) and K (23.0 GHz) bands were carried out in the D configuration on 1996 July 19 (with a bandwidth of 50 MHz), and in the Q band using the A configuration on 1996 December 26.

Table 1. Summary of the observations.

Name	Class	z	Tel	Date	λ_{obs} (μm)	λ_{rest} (μm)	t_{int} (s)	τ	S_ν (mJy)	S_ν/σ
TX 0211−122	RG	2.34	SEST	13 July 1995	1270	380	4500	0.19-0.22	-0.53±3.99	–
MRC 0943−242	RG	2.93	SEST	06 May 1996	1270	323	5500	0.11-0.13	4.33±3.29	1.3
MG 1019+0535	RG	2.76	IRAM	19-20 March 1996	1250	332	5760	0.30-0.40	2.13±0.47	4.5
MG 1019+0535	RG	2.76	JCMT	24 April 1996	790	210	10800	0.30-0.40	14.70±4.60	3.2
MRC 1043−291	RQ	2.13	SEST	07 May 1996	1270	406	800	0.15-0.17	29.38±8.15	3.6
1243+036	RG	3.58	JCMT	25 April 1996	790	172	14080	0.23-0.29	7.00±3.10	2.3
1243+036	RG	3.58	IRAM	19-20 March 1996	1250	273	2040	0.20-0.40	2.61±0.86	3.0
PKS 1251−407	RQ	4.46	SEST	07 May 1996	1270	233	3800	0.14-0.19	8.00±3.1	2.6
PKS 1354−107	RQ	3.00	SEST	06 May 1996	1270	317	2100	0.14-0.16	10.92±5.11	2.1

Note: RG – radio galaxy; RQ – radio-loud quasar; t_{int} – integration time on the source; τ – opacity during the observations.

The total on-source time was 10 minutes each in the X and U bands, and 20 m in the K band. The visibility averaging time was 10 s in all bands. The phase was calibrated with calibrator source 1024−008 which was observed every 10 m, and 3C 286 was observed as a flux calibrator. The data were reduced using standard AIPS procedures. The used synthesized beam sizes, are listed in Table 2. Maps with a cell size of 0.5″ were produced for each band. Maps were made and CLEANed using the MX routine within AIPS. The radio source was unresolved – no evidence was found for any extended emission. The total flux density, as measured from the maps in each band, is also given in Table 2. The major source of uncertainty for the measured flux density is the uncertainty in the flux scale, which we estimate to be of order 10%.

The Q band observation was carried out over a period of 1.7 hr using twelve VLA antennas. The total bandwidth for the observations was 100 MHz, centred at 43.34 GHz (6.9 mm). Again, the observing and calibration procedures were standard. After checking the pointing accuracy of the antennas, brief observations of MG 1019+0535 were sandwiched and interspersed with measurements of 1055+018, a bright, compact calibrator. The flux density of the galaxy was tied to that of the calibrator (4.62 Jy) which, in turn, was tied to the flux density of 3C 286 (1.49 Jy on the shortest baselines). The noise level at the position of the galaxy agreed well with that measured using the calibrated visibilities, giving a 3σ upper limit of 1.94 mJy.

Table 2. VLA observations of MG 1019+0535.

Date (1996)	ν_{obs} (GHz)	ν_{rest} (GHz)	Flux (mJy)	Config & Band	Beam size FWHM (″)
19 July	8.3	31.2	52.7±5.3	D,X	7.36×5.97
19 July	15.0	56.4	23.2±2.3	D,U	4.31×3.64
19 July	23.0	86.8	9.3±0.9	D,K	2.80×2.52
26 Dec	43.3	162.8	3σ <1.94	A,Q	–

3. Results

Table 1 shows the flux densities measured for our targets. The radio galaxy MG 1019+0535 is the only source detected at submillimetre wavelengths at greater than the 4-σ significance level. In this section we discuss the main implications of our observations for each individual source. The dust masses are estimated using the formula:

$$M_{\rm d} = \frac{S(\nu_{\rm obs}) D_{\rm L}^2}{(1+z)\kappa_{\rm d}(\nu_{\rm rest}) B(\nu_{\rm rest}, T_{\rm d})} \quad (1)$$

where S is the flux density, ν_{obs} and ν_{rest} are, respectively, the observed and rest-frame frequencies, $D_{\rm L}$ is the luminosity distance, B is the black-body Planck function, $T_{\rm d}$ is the dust temperature and $\kappa_{\rm d} = 0.67(\nu_{\rm rest}/250\,{\rm GHz})^2\,{\rm cm^2\,g^{-1}}$ is the adopted mass absorption coefficient. In order to obtain limits on $M_{\rm d}$, it is necessary to assume a temperature for the grains. We assume a representative temperature $T_{\rm d}$=60 K, consistent with the typical temperatures estimated for high-redshift active galaxies. For a discussion about the uncertainties of dust masses and temperatures, see Hughes et al. (1997). It should be emphasised here that, besides the uncertainties on $T_{\rm d}$ and $\kappa_{\rm d}$, the absolute dust masses are also strongly dependent on the choice of H_0 and q_0; in fact, they change by a factor of 4 for values of H_0 ranging from 50 to 100 km s^{-1} Mpc^{-1}, and by a factor of around 2 if q_0 is changed from $q_0 = 0.1$ to $q_0 = 0.5$.

For each source we have searched NED[1] in order to derive the spectral energy distributions (SEDs) over a broad range of frequencies. If the error of the flux density is unknown, we assume an uncertainty of 5%. Whenever the significance of the flux density is $\leq 3\sigma$, we provide an upper limit at the 3-σ level. Whenever more than one flux density value is available at the

[1] The NASA/IPAC Extragalactic Database (NED) is operated by the Jet Propulsion Laboratory, Caltech, under contract with the National Aeronautics and Space Administration.

Table 3. Flux densities.

Object	ν_{obs} (GHz)	Flux (mJy)	Ref	Object	ν_{obs} (GHz)	Flux (mJy)	Ref
TX 0211−122	0.408	1020±40	L81	MRC 1043−291	0.408	1090±60	L81
	1.465	189±9.5	C97		2.70	530±27	WO90
	4.70	53.8±5.0	C97		4.85	714±51	W96
	8.20	24.3±2.5	C97		5.00	320±16	WO90
	230	<12	here		230	<24.3	here
	4.61×10^5	$2.36\pm0.24\times10^{-3}$	vO94	1243+036	0.178	3600±180	WO90
MRC 0943−242	0.408	1050±30	L81		0.408	1810±80	L81
	1.50	245±13	C97		1.40	256±13.0	WB92
	4.70	56±3	C97		2.70	120±6.0	WO90
	4.85	44±11	Gri94		4.70	69.6±7.0	vO96
	8.20	21±1	C97		8.30	28.2±3.0	vO96
	230	<9.9	here		230	<2.6	here
	4.61×10^5	$5.93\pm0.59\times10^{-3}$	C97		384	<9.3	here
MG 1019+0535	0.178	2100±105	WO90		1.36×10^5	$1.28\pm0.13\times10^{-2}$	vO96
	0.365	925±31	D95		4.61×10^5	$2.84\pm0.28\times10^{-3}$	vO96
	0.408	920±50	L81	PKS 1251−407	0.33	<400	S96
	1.400	454±23	WB92		1.40	260±10	S96
	1.490	360±6	D95		2.70	250±10	S96
	2.700	180±9	WO90		4.85	238±15	W94
	4.850	100±12	Gri95		4.85	237±16	Gre94
	4.850	115±17	B91		4.90	200±10	S96
	4.850	132±19	Gre91		5.00	220±10	WO90
	8.333	52.7±5.3	here		15.0	110±10	S96
	8.439	59.1±1.5	D95		8.40	150±10	S96
	15.00	23.2±2.3	here		230	<9.3	here
	23.08	9.30±0.9	here		3.75×10^5	$2.47\pm0.25\times10^{-2}$	S96
	43.30	<1.94	here		6.82×10^5	$1.40\pm0.14\times10^{-3}$	vO96
	230.0	2.13±0.47	here	PKS 1354−107	2.70	260±13	WO90
	384.0	14.7±4.6	here		4.86	284±14	Gri94
	3000	<460	here		5.00	270±14	WO90
	5000	<200	here		8.40	280±14	S97
	1.20×10^4	<170	here		8.40	191±10	S97
	2.50×10^4	<110	here		230	<15.3	here
	1.36×10^5	$6.40\pm1.30\times10^{-3}$	D95				
	3.75×10^5	$1.70\pm0.17\times10^{-3}$	D95				
	4.61×10^5	$7.84\pm0.40\times10^{-4}$	D95				
	5.00×10^5	$5.05\pm0.50\times10^{-4}$	D95				
	6.00×10^5	$4.03\pm0.40\times10^{-4}$	D95				

Note: L81 – Large et al. (1981); C97 – Carilli et al. (1997); vO94 – van Ojik et al. (1994); Gri94 – Griffith et al. (1994); WO90 – Wright & Ostrupcek (1990); D95 – Dey et al. (1995); WB92 – White & Becker (1992); Gri95 – Griffith et al. (1995); B91 – Becker et al. (1991); Gre91 – Gregory & Condon (1991); W96 – Wright et al. (1996); vO96 – van Ojik et al. (1996); S96 – Shaver et al. (1996); S97 – Shaver et al. (in preparation); W94 – Wright et al. (1994); Gre94 – Gregory et al. (1994); Gri94 – Griffith et al. (1994).

same frequency, we plot all the available values. Figs. 1 and 2 and Table 3 show the SEDs derived for our targets.

3.1. Notes on individual sources

TX 0211−122

The optical emission line ratios of this radio galaxy are highly anomalous, with the flux of the Lyα line relatively weak, and that of the N Vλ1240 line relatively strong compared to those of C IVλ1549, He IIλ1640 and C III]λ1909 (van Ojik et al. 1994).

This was interpreted as being due to a strong starburst and a large amount of dust. According to the 8.2-GHz flux density and spectral index (Röttgering et al. 1994; Carilli et al. 1997), the expected synchrotron flux density at 1.3 mm is only $\sim$0.3 mJy. Our SEST observation yields a 3-σ upper limit of $\sim$12 mJy which limits the total amount of dust, according to Eq. (1), to $< 1.1 \times 10^9\,M_\odot$. Although this limit is not very stringent, it does suggest that the total amount of dust cannot be much larger than that of the most dusty known active galaxies: for instance, the quasar BRI 1202−0725 has $M_{\rm d} \sim 10^9\,M_\odot$ (Isaak et al. 1994; Hughes et al. 1997). Finally, we recall that the amount of molecular hydrogen estimated from observations of CO is $< 10^{11}\,M_\odot$; not much greater than that of nearby gas-rich starburst galaxies (van Ojik et al. 1997).

MRC 0943−242

The detection of a halo of neutral hydrogen linked with the host galaxy of MRC 0943−242 and the dust which might be associated with the neutral ISM (Röttgering et al. 1995) prompted the SEST observation of this source. We recall that the limit on the molecular hydrogen mass is $< 10^{11}\,M_\odot$ (van Ojik 1995). According to the 8.2-GHz flux density and spectral index (Röttgering et al. 1994; Carilli et al. 1997), the expected synchrotron flux density at 1.3 mm is only $\sim$0.2 mJy. Our 1.3-mm 3-σ upper limit of 9.9 mJy limits the mass of dust to $< 6.8 \times 10^8\,M_\odot$). Because of the large uncertainty in the total gas content (H+H_2) (Röttgering et al. 1995; van Ojik et al. 1997), it is not possible to meaningfully constrain the dust/gas mass ratio in this galaxy.

3.2. MG 1019+0535

This radio galaxy has spectroscopic properties similar to TX 0211−122, again indicating the possible presence of dust (Dey et al. 1995). Our IRAM observations provided a suggestive detection at 1.25 mm, and our JCMT observations yielded a marginal detection at 800 μm. The IRAM observations were split into two nights but in this case, unlike 1243+036, MG 1019+0535 gave consistently positive signal. Although the result is formally significant, we consider that our 1.25-mm data provide only a tentative detection because of the very weak flux density. We note, however, that previous IRAM detections at around this level have since proved to be trustworthy – that of 8C 1435+635, for example (Ivison 1995; Ivison et al. 1998).

It is important to stress that there are major uncertainties in the interpretation of the millimetric observations of this galaxy. Optical imaging shows the presence of two objects separated by about 1.5″ – object A, identified as the counterpart of the radio source at $z = 2.76$, and object B (Dey et al. 1995). The nature of B is unclear: it may be physically related to A, or be a foreground galaxy at $z \sim 0.66$. The problem is that the beam widths of our 1.25-mm and 800-μm observations include both objects. However, if the two objects are unrelated, the depression of the Lyα line favours component A being the dusty object and the source of the observed flux density at 1.3 mm.

In order to better constrain the SED of this galaxy, we used data from *IRAS*. However, since MG 1019+0535 is not detected, upper limits have been estimated at 12, 25, 60 and 100 μm by searching a 1 square degree field centred on MG 1019+0535 for sources from the *IRAS Faint Source Catalogue*, adopting the faintest in each band as the upper limit (0.11, 0.17, 0.20 and 0.47 Jy, respectively). This crude method relies on the fact that if the *FSC*'s sophisticated search routines cannot find a point source, then the source must be below the 3-σ threshold. The method is less prone than some to providing misleadingly low limits (Ivison 1995). The implication of this result is dicussed in detail in Sect. 4.

MRC 1043−291

This radio-loud quasar has radio flux densities of 1.09 and 0.68 Jy at 408 MHz and 5 GHz, respectively (Kapahi et al. 1997). Therefore, if we adopt a spectral index $\alpha = -0.19$ (defined as $S_\nu \propto \nu^\alpha$), we derive an expected 1.3-mm synchrotron flux density of around 326 mJy. Our SEST observation provides a flux density around an order of magnitude lower than expected, suggesting that the radio spectrum steepens rapidly at high frequencies.

1243+036 (= 4C 03.24)

This is the radio galaxy with the highest redshift in our observed sample. One spectacular feature is the presence of a Lyα halo (with a luminosity of $\simeq 10^{44}\,{\rm erg\,s^{-1}}$) which extends over 20″ ($\simeq$ 135 kpc) (van Ojik et al. 1996). The Lyα images, coupled with high-resolution spectra, indicate that the radio jet is interacting vigorously with the gas in the inner region. Perhaps most surprising is the low-surface-brightness outer region of the Lyα halo. Deep spectroscopy shows that it is relatively quiescent ($\simeq 250\,{\rm km\,s^{-1}}$ FWHM), but that there is a velocity gradient of $450\,{\rm km\,s^{-1}}$ over the extent of the emission ($\simeq$ 135 kpc). Because the halo extends beyond the radio source, it is probable that its kinematics must predate the radio source. The ordered motion may be a large-scale rotation caused by the accretion of gas from the environment of the radio galaxy or by a merger.

The extrapolation of the radio flux density at 8.3 GHz (Röttgering et al. 1994; van Ojik et al. 1996) provides expected synchrotron flux densities of 0.2 and 0.4 mJy, respectively, at 800 μm and 1.3 mm. We observed this source, both with the IRAM telescope and the JCMT, but we obtained only non-significant detections at the 2-3-σ level (see Table 1). The IRAM observations were performed on two different nights. Although the combined observations of the two nights provide a formal 3-σ detection, we found that this result is not reliable because the source was detected only during the first night. In fact, deeper observations with the IRAM telescope failed to detect the galaxy and provided a 3-σ upper limit $<$ 1.5 mJy (R. Chini, private communication).

However, we can see that our 3-σ upper limits ($<$9.3 mJy at 800 μm; $<$2.6 mJy at 1.3 mm) provide a relevant result. In fact, the inferred total dust masses are $< 1.0 \times 10^8$ and

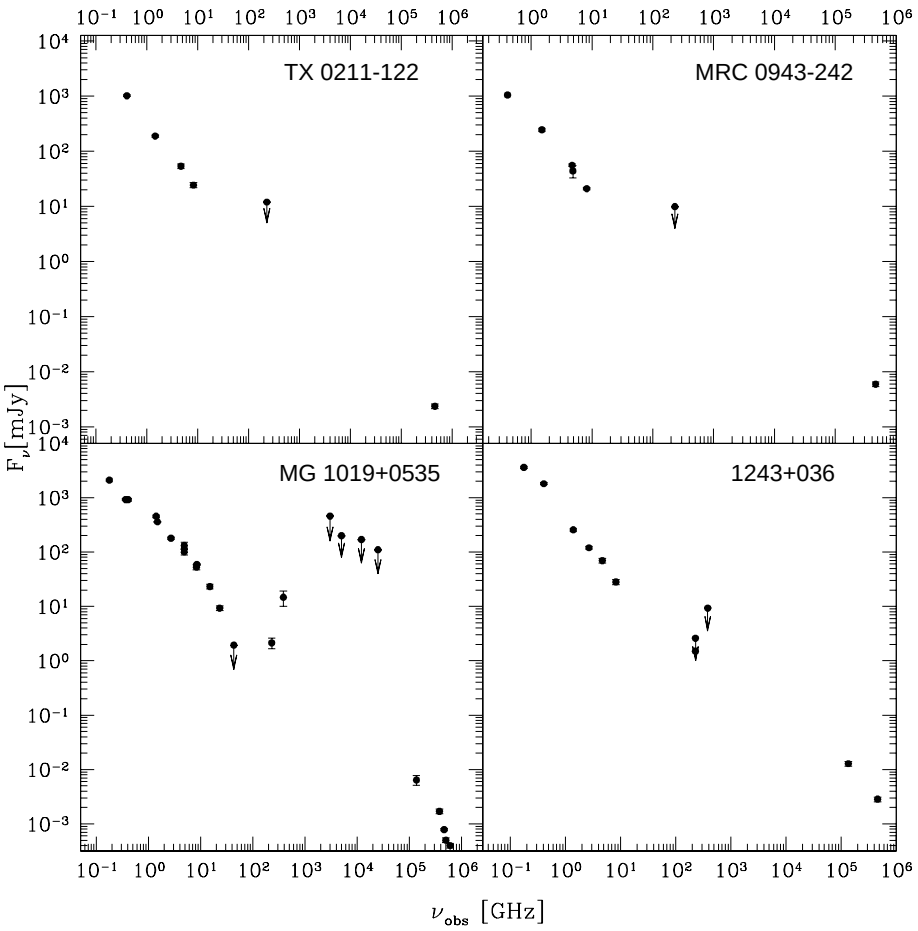

Fig. 1. Spectral energy distributions of radio galaxies. The flux densities and the relative references are listed in Table 3.

$< 1.3 \times 10^8\,M_\odot$ using the 800-μm and 1.3-mm upper limits, respectively. The most stringent limit on the dust mass (provided by the JCMT observation) implies that the amount of dust in 1243+036 is lower than that inferred for those high-z radio galaxies and quasars so far detected (see Hughes et al. 1997 and references therein). The upper limit on $M_{\rm d}$ can be lowered still further if we use the limit provided by Chini at 1.3 mm, which gives $M_{\rm d} < 7.7 \times 10^7\,M_\odot$. It is also important to notice that CO observations of this galaxy have provided a stringent limit on the amount of molecular hydrogen $< 5 \times 10^{10}\,M_\odot$ (van Ojik 1995).

PKS 1251−407

To date, this is the furthest known radio-loud quasar (Shaver et al. 1996). Our SEST observation provides a tentative (2.6-σ) detection. Fig. 2 shows the SED of this quasar. The 1.3-mm upper limit hints that the synchrotron spectrum steepens at high frequencies, as do the other two radio-loud quasars, MRC 1043−291 and PKS 1354−107.

PKS 1354−107

The optical counterpart of this radio source was identified by Shaver et al. (P.A. Shaver, J.V. Wall, K.I. Kellermann, C.A. Jackson, M.R.S. Hawkins, private communication) with a quasar at z = 3.0. The available radio flux densities (see Fig. 2) suggest the presence of a very flat spectrum from 2.7 to 8.4 GHz. Our SEST observation provides a 3-σ upper limit of <15.3 mJy, implying a sharp steepening of the synchrotron spectrum at high frequencies.

4. The case of MG 1019+0535: a dusty radio galaxy

Although the JCMT observation provides only a marginal detection, its combination with the IRAM detection of an excess over the synchrotron spectrum strongly suggests the presence of thermal dust emission from this galaxy (Fig. 3).

Hughes et al. (1997) have demonstrated that the uncertainties in calculating the mass of dust responsible for the optically thin, thermal, submillimetre emission are: (i) our limited knowledge of the rest-frame mass absorption coefficient, $\kappa_{\rm d}$, and how this quantity varies with frequency; (ii) the dust temperature ($T_{\rm d}$), and, finally, (iii) the unknown values of H_0 and q_0. Unfortunately, these problems are coupled. For example, Hughes et al. (1993) noted that there is a trade off between $T_{\rm d}$ and the critical frequency at which the dust becomes optically thick, ν_0.

Typically, each of these uncertainties can account for changes of up to a factor $\sim$ 5 in derived dust masses (see Hughes et al. 1997 for more details). However, a conservative

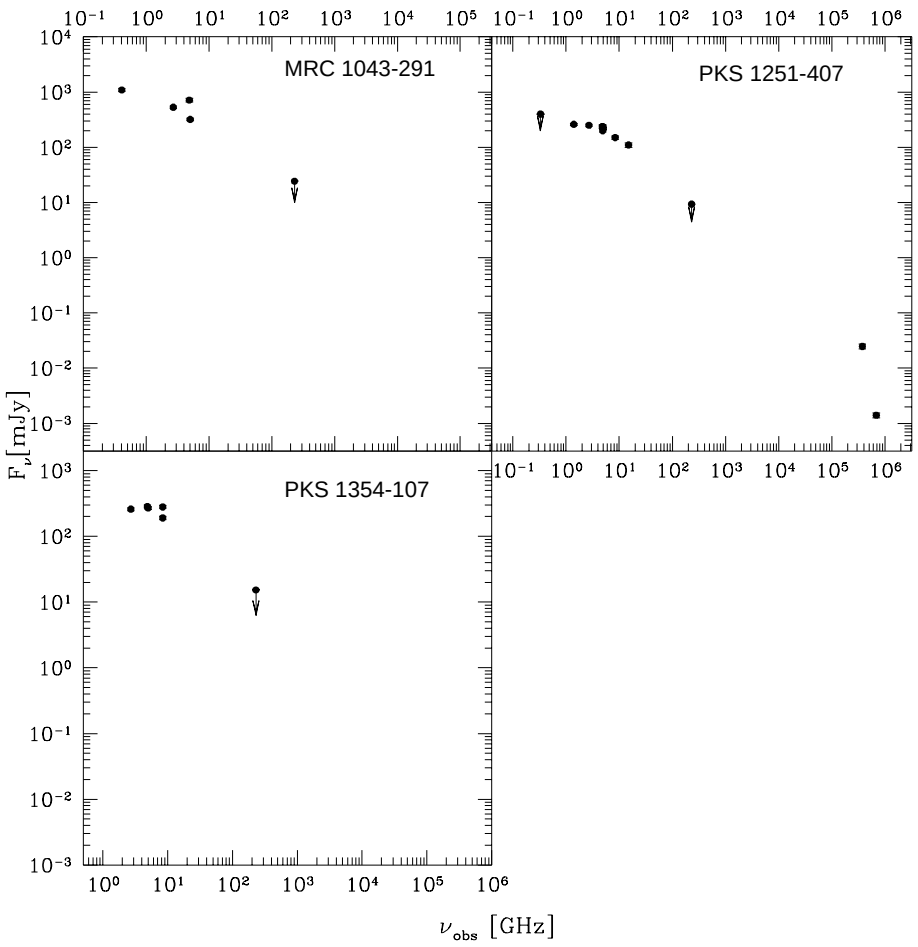

Fig. 2. Spectral energy distributions of radio-loud quasars. The flux densities and the relative references are listed in Table 3.

value for the dust mass can be obtained if the paramaters we use to estimate the dust mass are taken such that the dust mass is minimised. We further note that (since for high-z objects the submillimetre observations sample the Rayleigh-Jeans region) the slope of the dust spectrum is not a function of temperature.

Our measurements of MG 1019+0535 at 240 and 384 GHz suggest that the submillimetre spectral index (α, where $S_\nu \propto \nu^\alpha$) is large and positive (α = +4.2 $\pm$ 1.2). We recall that the maximum allowed spectral index for self-absorption is +2.5. Our result therefore rules out the possibility that the emission is due to self-absorbed synchrotron radiation (Chini et al. 1989). However, given the uncertainty of the 384-GHz flux density, data at more frequencies are needed to better constrain α.

Strong support for the thermal nature of the submillimetre emission is provided by our deep measurements at 22 and 43 GHz using the VLA. These show that the steepening centimetre spectral index (Figs. 1 and 3) becomes still more negative as it approaches the millimetre domaine; the predicted contribution at 240 GHz from the dominant centimetre component lies several orders of magnitude below the measured 240-GHz flux density.

At first sight this indicates that the frequency dependence of the dust grain emissivity (or the emissivity index, β) is +2.2 $\pm$ 1.2, which encompasses the range normally quoted for interstellar grains ($1.0 < \beta < 2.0$) as well as some less physical values ($\beta > 2.0$). However, the redshift is high and the rest-frame frequency of the observed 374-GHz emission is close to the turnover of the dust spectrum, so we do in fact require a high value of β to fit both the 240- and 384-GHz data. For β = +2.0, we find that $35 < T_{\rm d}/{\rm K} < 180$. The lowest temperatures (35 K) are found for an optically thin solution; the highest temperature (180 K) is permitted when we allow the dust to become optically thick (say at ν_0 = 1.5 THz or 200 μm) and to be constrained by the *IRAS* upper limits.

Although it is clear that our observations do not constrain stringently the dust temperature, we can make use of the usual theory (Hughes et al. 1997) to estimate the mass of dust responsible for the emission detected by IRAM and JCMT. For $35 < T_{\rm d}/{\rm K} < 180$, $0.17 < M_{\rm d}/10^8\,{\rm M}_\odot < 1.8$.

It is reassuring that $T_{\rm d}$ = 40 K is viable since this is the temperature of the dust measured in the z = 4.25 radio galaxy, 8C 1435+635 (Ivison et al. 1998). For $T_{\rm d}$ = 40 K, adopting the same dust parameters as Ivison et al., we derive $M_{\rm d} = 2 \times 10^8 h_{50}^{-2}\,{\rm M}_\odot$ which, when compared with the dust mass estimate of $4 \times 10^8 h_{50}^{-2}\,{\rm M}_\odot$ for 8C 1435+635, suggests that the dust mass in powerful radio galaxies does not change significantly between z = 4.25 and 2.76 (though we note that the rest-frame 6-cm luminosity of 8C 1435+635 is around 5 times

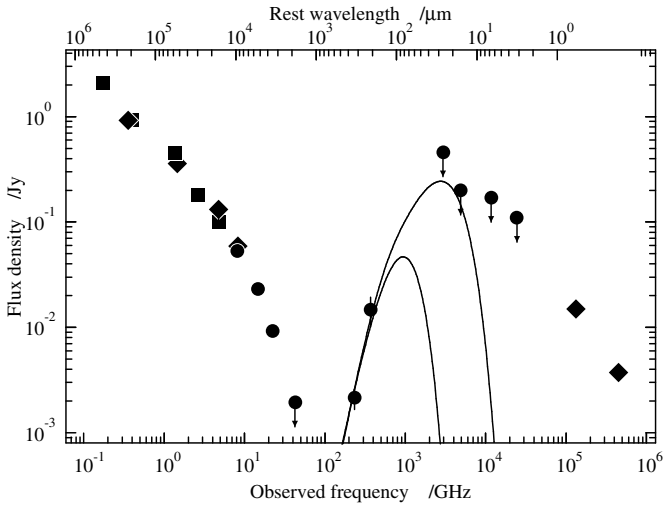

Fig. 3. Spectral energy distribution of MG 1019+0535. The lines drawn in the rest-frame far-IR are modified 35- and 180-K blackbodies, with a β=+2 frequency dependence for the dust-grain emissivity, representing the most extreme dust temperatures compatible with our data. The 180-K blackbody is optically thick at 200 μm. Key: circles – VLA, JCMT, IRAM and *IRAS* measurements described in the text; diamonds – measurements from Dey et al. (1995); squares – measurements from Griffith et al. (1995), Becker, White & Edwards (1991), Wright & Otrupcek (1990) and White & Becker (1992).

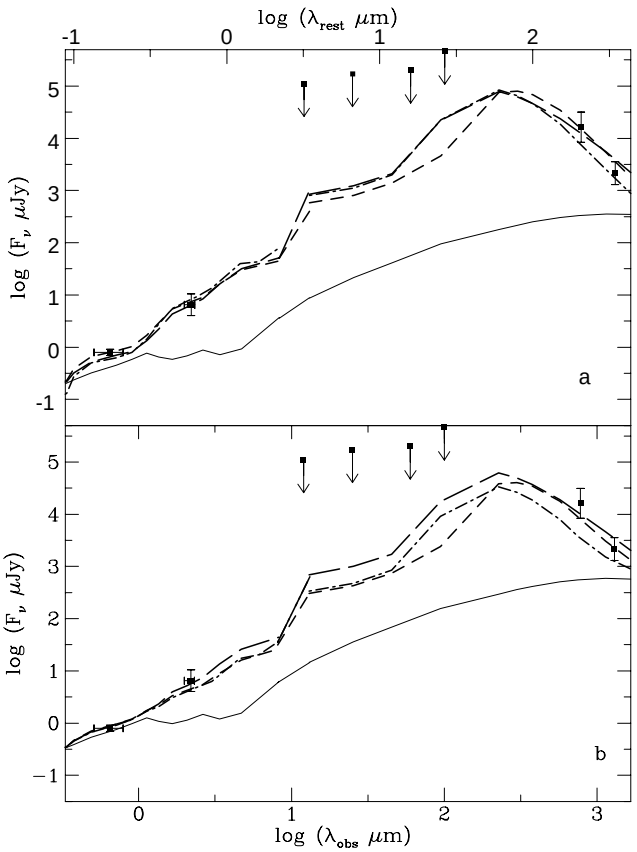

Fig. 4a and b. The fits to the SED of MG 1019+0535 as obtained with the Mazzei & De Zotti (1996) model. Thick lines correspond to the overall match of the SED of MG 1019+0535 for models including a non thermal contribution, stellar emission and dust effects (see text); **a** shows the results for two models corresponding to a host galaxy 1-Gyr old, short-dashed (m_l = 0.01 $M_\odot$) and long-dashed lines (m_l = 0.5 $M_\odot$), with a non-thermal contribution at 0.64 μm of 70 and 80% respectively (thin line); the overall match for a host galaxy 0.8-Gyr old (dot-dashed line, m_l = 0.1 $M_\odot$) with a non-thermal contribution of 50% at the same wavelength is also shown; in **b** are the results for the same models raising the non-thermal contribution at the same wavelength to 90%; short-dashed curves require a dust temperature of 46 K instead of 60 K.

that of MG 1019+0535 and that observations of complete samples of radio galaxies spanning a range of redshifts and radio luminosities will be required to trace their evolution in detail).

4.1. Modelling the UV-to-FIR SED

The interpretation of the observed spectral energy distributions (SEDs), is not straightforward, since a non-thermal contribution cannot be neglected and the commonly used population synthesis models do not allow for dust extinction. Using the same approach followed by Mazzei & De Zotti (1996), based on chemo-photometric population synthesis models incorporating extinction and re-emission by dust and accounting for non-thermal emission, we have attempted to analyse the SED of MG 1019+0535. We recall here that Dey et al. (1995) estimate an upper limit to the internal reddening, $E_{B-V} < 0.43$ mag.

Our IRAM (and, marginally, JCMT) observations strongly favour the presence of dust. Although our spectral coverage is rather poor, we attempt to fit the overall SED of this galaxy, from the optical to 1.25 mm in the observed frame, with the aim of constraining the evolutionary properties of MG 1019+0535. For this study, we assume that the source of the submillimetre continuum radiation is component A (as suggested by its depleted Lyα emission), and we adopt its optical and near-IR fluxes accordingly (Dey et al. 1995).

We have computed several models with Salpeter's initial mass function (IMF) and different lower mass limits, m_l, as described in Mazzei & De Zotti (1996) (and references therein). For a given model we derive the age of the system which matches the data, with different amounts of non-thermal AGN emission. We find an interesting result: these data are well matched by models which always correspond to a 0.8-1-Gyr-old host galaxy, accounting for a non-thermal contribution ranging from 50 to 90% of the total flux density at 0.6 μm (see Fig. 4). According to this result, MG 1019+0535 cannot be considered a "primaeval" galaxy candidate because the bulk of its stellar population is significantly evolved. For H_0 = 50 km s^{-1} Mpc^{-1}, the formation redshift, $z_{\rm form}$, of MG 1019+0535 is between 10 and 4 if q_0 = 0.5 and < 5 if q_0 = 0. In the following we will refer to the first value of q_0.

The expected bolometric luminosity is always larger than 10^{13} $L_\odot$; in particular, this rises by a factor 2.5 if m_l = 0.5 $M_\odot$. This corresponds to a residual gas fraction of 2%, i.e. to a total gas mass of about 4×10^{10} M$_\odot$, which is well below the Evans et

al. (1996) upper limit, with E_{B-V} = 0.13, a total barionic mass, $M_{\rm barion}$, of around $1.7 \times 10^{12}\,{\rm M}_\odot$, and a star-formation rate of $800\,{\rm M}_\odot\,{\rm yr}^{-1}$. In this scenario, the hot stars are almost completely obscured by dust which, heated by their radiation field, transfers their bolometric luminosity to the far-IR wavelength regime. Models with lower m_l require larger $M_{\rm barion}$ and higher star-formation rates. We derive $E_{B-V} \leq 0.26$ for a residual gas fraction as large as 30% – the largest allowed by models – and $M_{\rm barion} < 4.5 \times 10^{12}\,M_\odot$.

The available data can be fully accounted for by opaque models like those already used by Mazzei & De Zotti (1994) to fit the spectrum of the ultraluminous galaxy IRAS $F10214+4724$. However, there is still considerable latitude for modelling. Crucial constraints may be provided by ground-based submillimetre measurements and by observations with the *Infrared Space Observatory (ISO)*; these measurements will help to define the shape of the far-IR SED, so settling the dust temperature, and the role of PAHs in the near-IR spectral range.

5. Results on radio-loud quasars

The three quasars show a sharp steepening of their synchrotron spectra between rest-frame radio and submillimetre wavelengths. It is important to recall that variability may affect the flux densities of radio-loud quasars obtained at different epochs. In order to estimate the magnitude of the spectral break in the millimetre region, we evaluate the expected synchrotron flux density at $\nu_{\rm obs}$=230 GHz, deriving the spectral index from the available data and extrapolating the 5-GHz radio flux densities to 1.3 mm. If two flux densities are available at the same frequency, we adopt the average value. For PKS 1251−407, we use only the quasi-simultaneous 1.4-15-GHz data of Shaver et al. (1996). For MRC 1043−291, we find that $\alpha(0.408 - 5\,{\rm GHz}) = -0.32$, and that the expected flux density at 230 GHz is $S_{\rm exp}(230) \sim 152$ mJy. For PKS 1251−407 and PKS 1354−107, we find $\alpha(1.4 - 15\,{\rm GHz}) = -0.37$, $\alpha(2.7 - 8.4\,{\rm GHz}) = -0.07$, with $S_{\rm exp}(230) \sim 50$ mJy and $S_{\rm exp}(230) \sim 210$ mJy, respectively. If we compare the expected flux densities with the observed upper limits, we find that $S_{\rm exp}(230)/S_{\rm obs}(230) > 5 - 14$, i.e. the observed flux density can be more than an order of magnitude lower than expected. We cannot know what fraction of this cut-off *may* be due to variability; however, the typical maximum amplitude of the variability of flat-spectrum radio sources at $\lambda \sim 1$ mm-11 cm, over timescales of months-years, is 40-60% (Jones et al. 1981 and references therein). It therefore seems unlikely that variability alone can explain the sharp cut-offs observed in the three quasars in our sample.

Moreover, high-frequency spectral turnovers have been often observed in radio-loud quasars at lower redshifts (Chini et al. 1989; Antonucci, Barvainis & Alloin 1990; Klein et al. 1996). In particular, the spectral break occurs in radio-loud quasars with either flat or steep radio spectra, whereas in BL Lac objects the submillimetre flux densities lie on an extrapolation of the radio spectrum (Knapp & Patten 1991). Our observations show a turnover at $\log\nu_{\rm rest}({\rm Hz}) \leq 11.8 - 12$, but the lack of further spectral information does not allow us to infer whether the steepening of the synchrotron-sub-mm spectra is related to thermal emission from dust peaking at the higher frequencies. It is important to recall that the question of dust in high-redshift, radio-loud quasars is very relevant to unification models (see Baker & Hunstead 1995 for a discussion of dust in radio-loud quasars) and to test the hypothesis that many quasars may be missed in optical surveys (see Webster et al. 1995). Future observations with *ISO* and SCUBA will extend the SED coverage to higher frequencies for a large number of objects.

6. Concluding remarks

We have presented observations of the rest-frame far-infrared continuum of a small sample of radio-loud AGN (4 radio galaxies and 3 quasars) with $2 < z < 4.5$.

One of the main findings is the detection of thermal continuum emission from the radio galaxy MG 1019+0535 ($z \sim 2.8$). This is particularly important since it confirms the suggestion that its weak Lyα emission is probably due to dust extinction. We attempt to estimate the temperature of the dust in order to derive the dust total mass, but the present data data do not allow us to constrain stringently the range of possible temperatures. However, we estimate that the total dust mass should be of order $0.2 - 2.0 \times 10^8\,{\rm M}_\odot$ for temperatures $T_{\rm d} \sim 35 - 180$ K. The overall rest-frame UV-FIR SED can be accounted for by a relatively evolved host galaxy (age ∼0.8 Gyr) experiencing an episode of vigorous star formation.

The radio galaxy 1243+036 ($z \sim 3.6$), on the other hand, seems to have a lower amount of dust and molecular gas than those active galaxies that have so far been detected at high redshifts, indicating that the properties of the ISM in active objects at $z > 2$ can be rather inhomogeneous.

Finally, the three flat-spectrum radio-loud quasars ($2 < z < 4.5$) observed at 1.3 mm show evidence of a spectral turnover at high frequencies. Our data do not allow us to understand what fraction of the turnover is due to the effects of variability, but we conclude that variability cannot be the only cause.

Acknowledgements. We acknowledge the referee, A. Omont, for the useful suggestions. We thank Raphael Moreno and Goeran Sandell who did some of the observations in service mode at the IRAM and JCMT telescopes respectively, and Roberto Fanti for useful discussions. This work was supported in part by the Formation and Evolution of Galaxies network set up by the European Commission under contract ERB FMRX-CT96-086 of its TMR programme and by the high-z programme subsidy granted by the Netherlands Organization for Scientific Research (NWO). RJI is supported by a PPARC Advanced Fellowship.

References

Andreani P., La Franca F., Cristiani S. 1993, MNRAS, 261, L35
Andreani P. 1994, ApJ, 428, 447
Antonucci R., Barvainis R., Alloin D. 1990, ApJ, 353, 416
Baker J.C., Hunstead R.W. 1995, ApJ, 452, L95
Becker R.M., White R.L., Edwards A.L. 1991, ApJS, 75, 1
Carilli C.L., Röttgering H.J.A., van Ojik R., Miley G.K., van Breugel W.J.M. 1997, ApJS, 109, 1

Chini R., Biermann P.L., Kreysa E., Gemünd H.-P. 1989, A&A, 221, L3
Cimatti A., Freudling W. 1995, A&A, 300, 360
Cimatti A. 1996, in "New Extragalactic Perspectives in the New South Africa – Changing Perceptions of the Morphology, Dust Content and Dust-Gas Ratios in Galaxies", ed. D. Block, Kluwer Academic Publisher, in press.
Dey A., Spinrad H., Dickinson M. 1995, ApJ, 440, 515
Downes D., Radford S.J.E., Greve A., Thum C., Solomon P.M., Wink J.E. 1992, ApJ, 398, L25
Downes D., Solomon P.M., Sanders D.B., Evans A.S. 1996, A&A, 313, 91
Duncan W.D. et al. 1990, MNRAS, 243, 126
Eales S.A., Edmunds M.G. 1996, MNRAS, 280, 1167
Evans A.S., Sanders D.B., Mazzarella J.M., Solomon P.M., Downes D., Kramer C., Radford S.J.E. 1996, ApJ, 457, 658
Gregory P.C., Condon J.J. 1991, ApJS, 75, 1011
Gregory P.C., Vavasour J.D., Scott W.K., Condon J.J. 1994, ApJS, 90, 173
Griffith M.R., Wright A.E., Burke B.F., Ekers R.D. 1994, ApJS, 90, 179
Griffith M.R., Wright A.E., Burke B.F., Ekers R.D. 1995, ApJS, 97, 347
Hu E.M., Ridgway S.E. 1994, AJ, 107, 1303
Hughes D.H., Robson E.I., Dunlop J.S., Gear W.K. 1993, MNRAS, 263, 607
Hughes D.H., Dunlop J.S., Rawlings S. 1997, MNRAS, 289, 766
Isaak K.G., McMahon R.G., Hills R.E., Withington S. 1994, MNRAS, 269, L28
Ivison R.J. 1995, MNRAS, 275, L33
Ivison R.J. et al., 1998, ApJ, submitted
Jones T.W., Rudnick L., Owen F.N., Puschell J.J., Ennis D.J., Werner M.N. 1981, ApJ, 243, 97
Klein U., Vigotti M., Gregorini L., Reuter H.-P., Mack K.-H., Fanti R. 1996, A&A, 313, 417
Knapp G.R., Patten B.M. 1991, AJ, 101, 1609
Large M.I., Mills B.Y., Little A.G., Crawford D.F., Sutton J.M. 1981, MNRAS, 194, 693
Mazzei P., De Zotti G. 1994, MNRAS, 266, L5
Mazzei P., De Zotti G. 1996, MNRAS, 279, 535
Kapahi V.K., Athreya R.M., Subrahmanya C.R., Baker J.C., Hunstead R.W., McCarthy P.J., van Breugel W. 1997, ApJS, submitted
Ohta K., Yamada T., Nakanishi K., Kohno K., Akiyama M., Kawabe R. 1996, Nature, 382, 426
Omont A., Petitjean P., Guilloteau S., McMahon R.G., Solomon P.M., Pecontal E. 1996a, Nature, 382, 428
Omont A., McMahon R. G.; Cox P., Kreysa E., Bergeron J., Pajot F., Storrie-Lombardi L.J. 1996b, A&A, 315, 10
Pei Y.C., Fall S.M., Bechtold J. 1991, ApJ, 378, 6
Pettini M.S., Smith L.J., Hunstead R.W., King D.L. 1994, ApJ, 426, 79
Röttgering H.J.A., Lacy M., Miley G., Chambers K., Saunders R. 1994, A&A 108, 79
Röttgering H.J.A, Hunstead R.W., Miley G.K., van Ojik R., Wieringa M.H. 1995, MNRAS, 277, 389
Sandell G. 1994, MNRAS, 271, 75
Shaver P.A., Wall J.V., Kellermann K.I. 1996, MNRAS, 278, L11
Smail I.R., Ivison R.J., Blain A.W., 1997, ApJ, submitted
van Ojik R., Röttgering H.J.A., Bremer M.N., Macchetto F., Chambers K.C. 1994, A&A, 289, 54
van Ojik R., Röttgering H.J.A., van der Werf P.P., Miley G.K., Carilli C.L., Isaak K., Lacy M., Jenness T., Sleath J., Visser A., Wink J. 1997, A&A in press
van Ojik R., Röttgering H.J.A., Carilli C.L., Miley G.K., Bremer M.N., Macchetto F. 1996, A&A, 313, 25
Webster R.L., Francis P.J., Peterson B.A., Drinkwater M.J., Masci F.J. 1995, Nature, 375, 469
White R.L., Becker R.M. 1991, ApJS, 79, 331
Wright A., Ostrupcek R. 1990, Parkes Catalogue, Australia National Telescope Facility.
Wright A.E., Griffith M.R., Burke B.F., Ekers R.D. 1994, ApJS, 91, 111
Wright A.E., Griffith M.R., Hunt A.J., Troup E., Burke B.F., Ekers R.D. 1996, ApJS, 103, 145

This article was processed by the author using Springer-Verlag LaTeX A&A style file *L-AA* version 3.